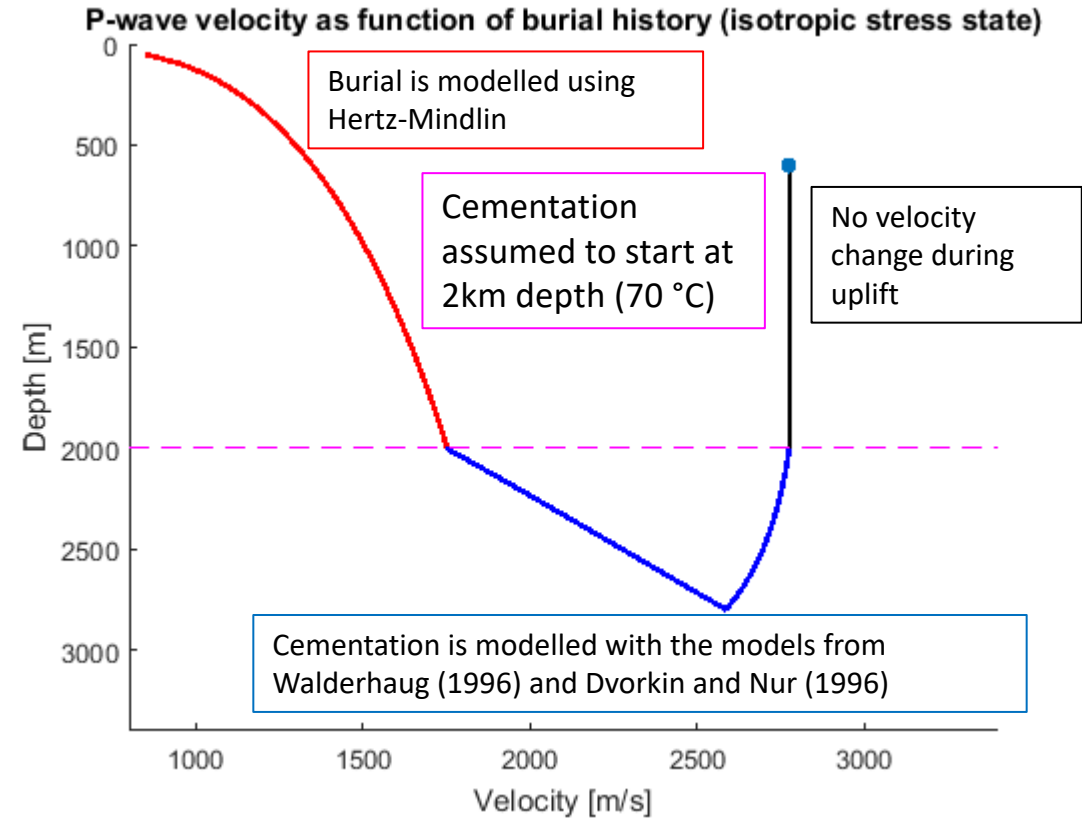# Laboratory Measurements as a Tool in Rock Physics Modelling of Uplift
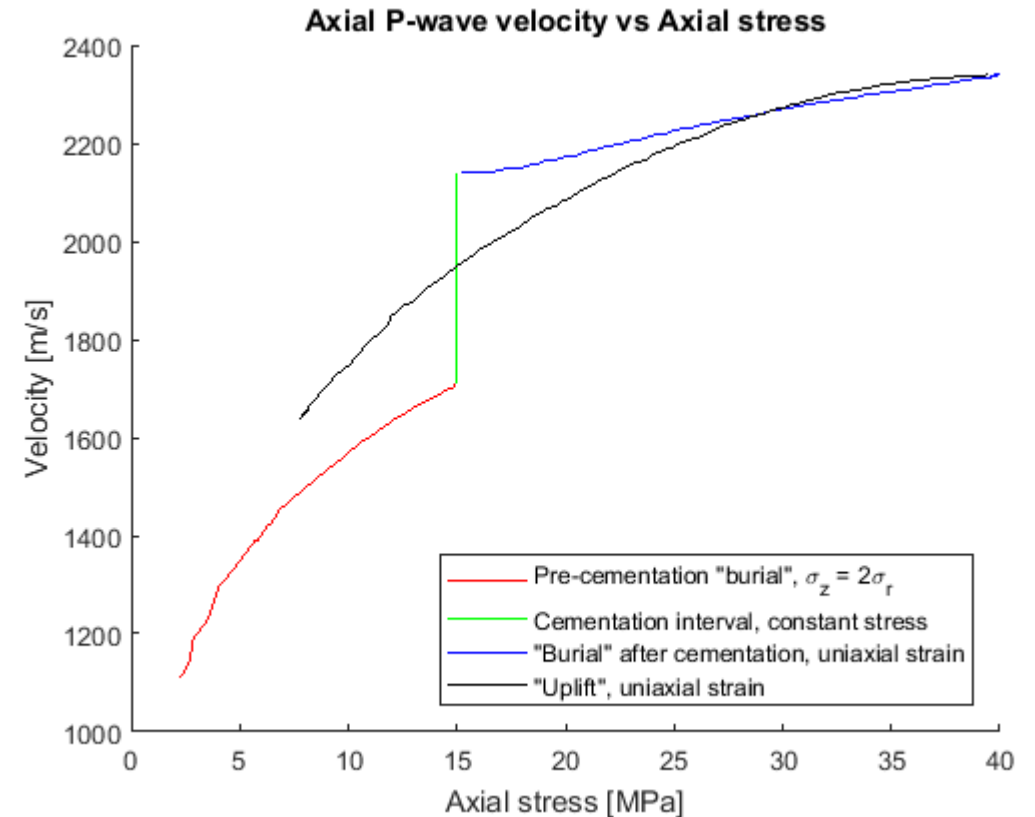
Sondre Torset – Student, NTNU

Conceptual Model

- A dry velocity of 2776m/s is measured at 600 m depth
- Granular media models (In this case Hertz-Mindlin) and cementation models (In this case Walderhaug and Dvorkin Nur) can be used to model velocity increase with depth.
- Max burial predicted by this result: 2800m

P-wave velocity as function of burial history (isotropic stress state)

Burial is modelled using Hertz-Mindlin

Cementation assumed to start at 2km depth (70 °C)

No velocity change during uplift

Cementation is modelled with the models from Walderhaug (1996) and Dvorkin and Nur (1996)

Experimental data

- SINTEF conducted experiments with loading and unloading of synthetic sandstones formed under stress.

- Clear increase in stress dependence upon unloading

- After the cementation the sample seems to retain some stress dependence.

- Not a lot of cement

Axial P-wave velocity vs Axial stress

Legend:
- Pre-cementation "burial", $\sigma_z = 2\sigma_r$
- Cementation interval, constant stress
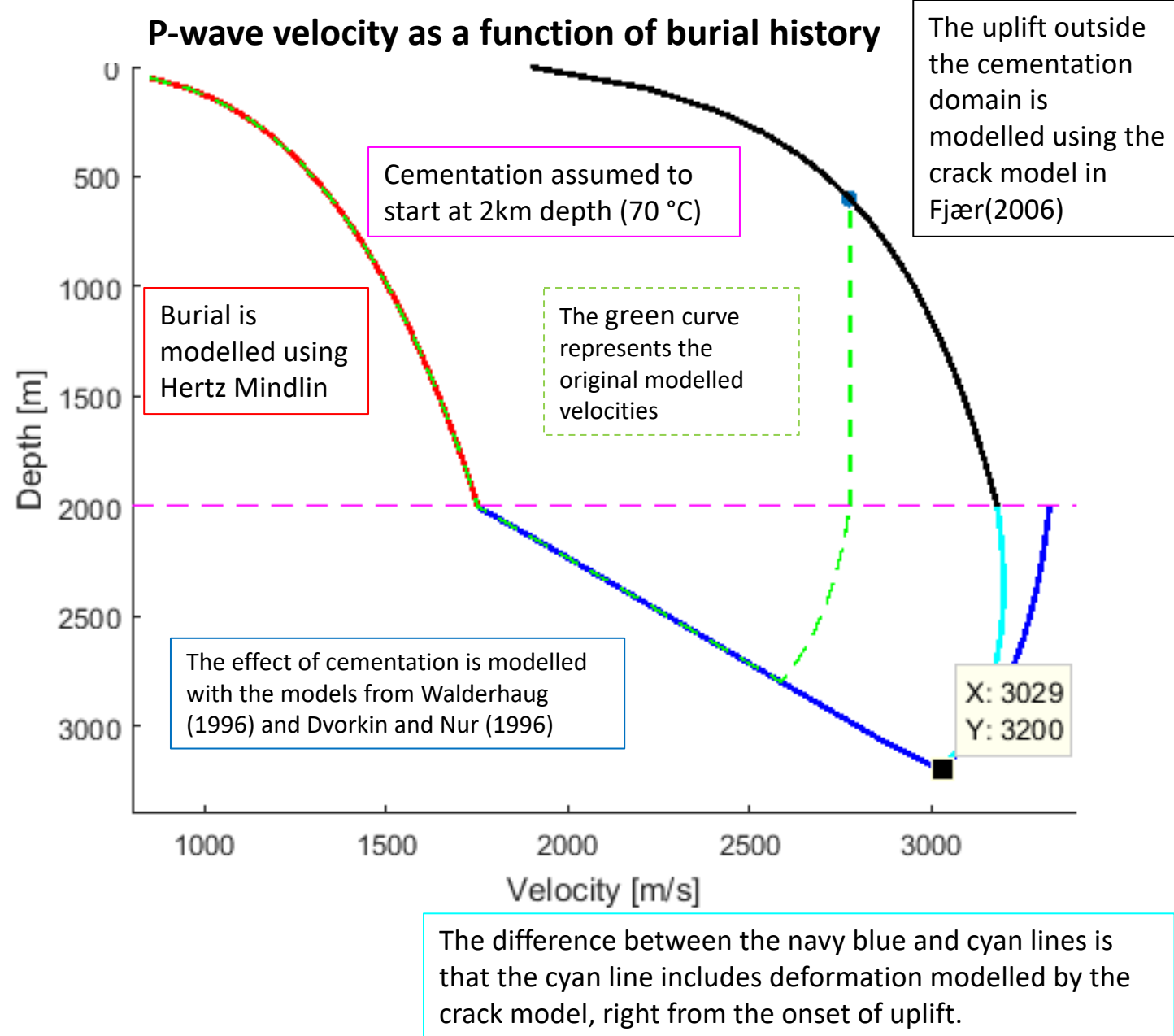- "Burial" after cementation, uniaxial strain
- "Uplift", uniaxial strain

If the experimental data are taken to be a fair representation of the subsurface, the methodology presented previously will over predict velocities, and thus under predict uplift.

See Holt et al. (2014) for a more detailed explanation of the experimental procedure

Updated Conceptual Model

- The laboratory data suggests a reduced velocity as a result of the uplift

- To obtain the observed velocity at 600m, the rock will therefore have to be buried deeper

- Uplift is under predicted by 400 meters in this illustration

- The actual effect of the uplift is likely to be case dependent

- This figure is just meant to serve as an illustration of the concept.

P-wave velocity as a function of burial history

The uplift outside the cementation domain is modelled using the crack model in Fjær(2006)

Cementation assumed to start at 2km depth (70 °C)

Burial is modelled using Hertz Mindlin

The green curve represents the original modelled velocities

The effect of cementation is modelled with the models from Walderhaug (1996) and Dvorkin and Nur (1996)

X: 3029
Y: 3200

The difference between the navy blue and cyan lines is that the cyan line includes deformation modelled by the crack model, right from the onset of uplift.

Anisotropy in the laboratory data

- P-wave anisotropy is also preserved after cementation, although it is reduced

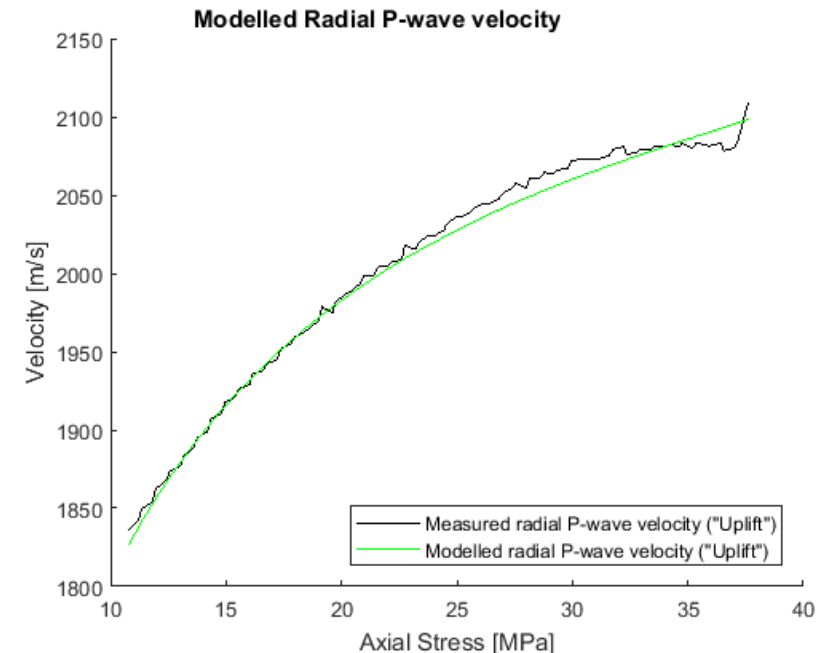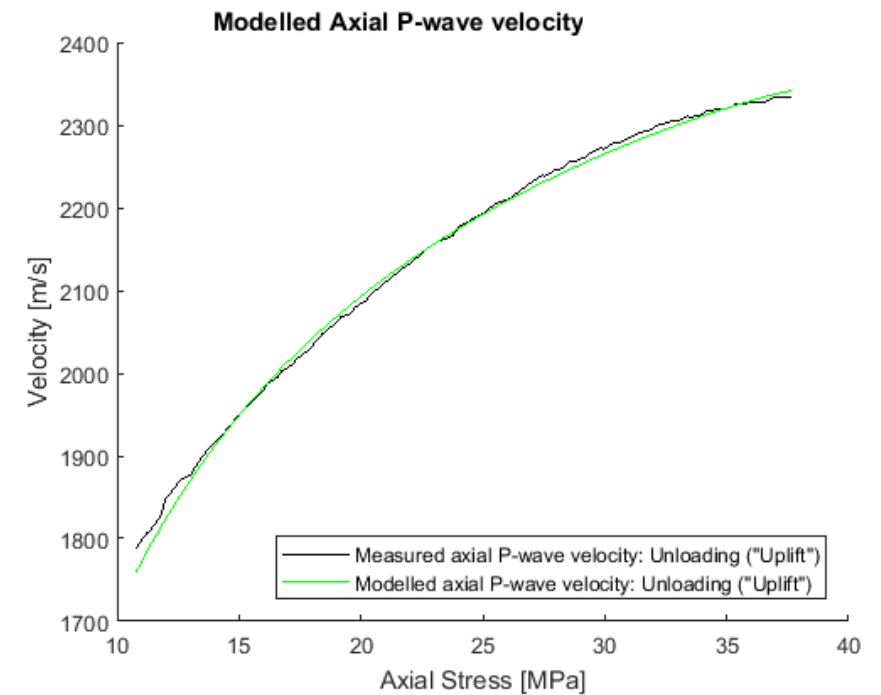- Upon uplift the P-wave anisotropy shows a distinctly different behavior compared to loading
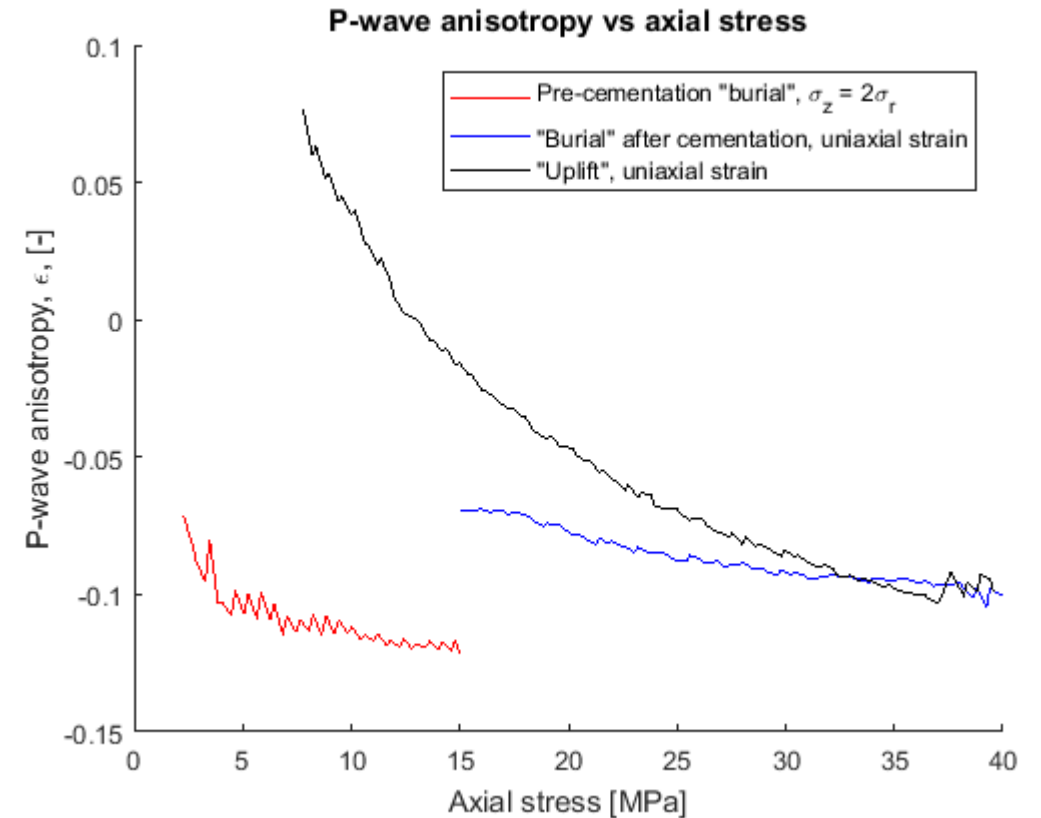
Can the anisotropy and stress dependence of P-wave velocities be modelled throughout the "burial history" of the synthetic sandstone?

See Holt et al. (2014) for a more detailed explanation of the experimental procedure
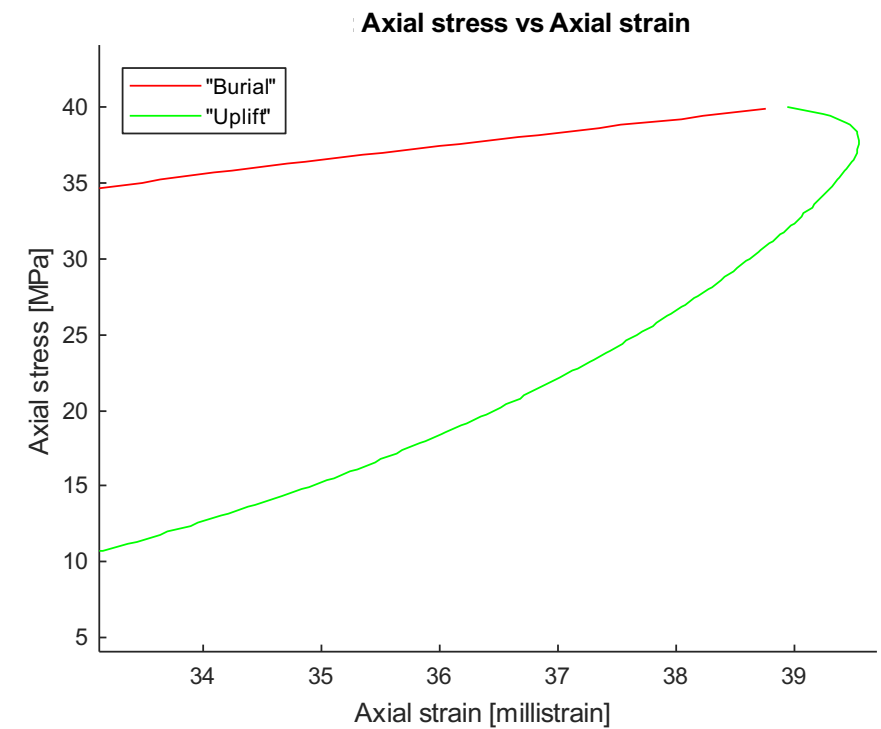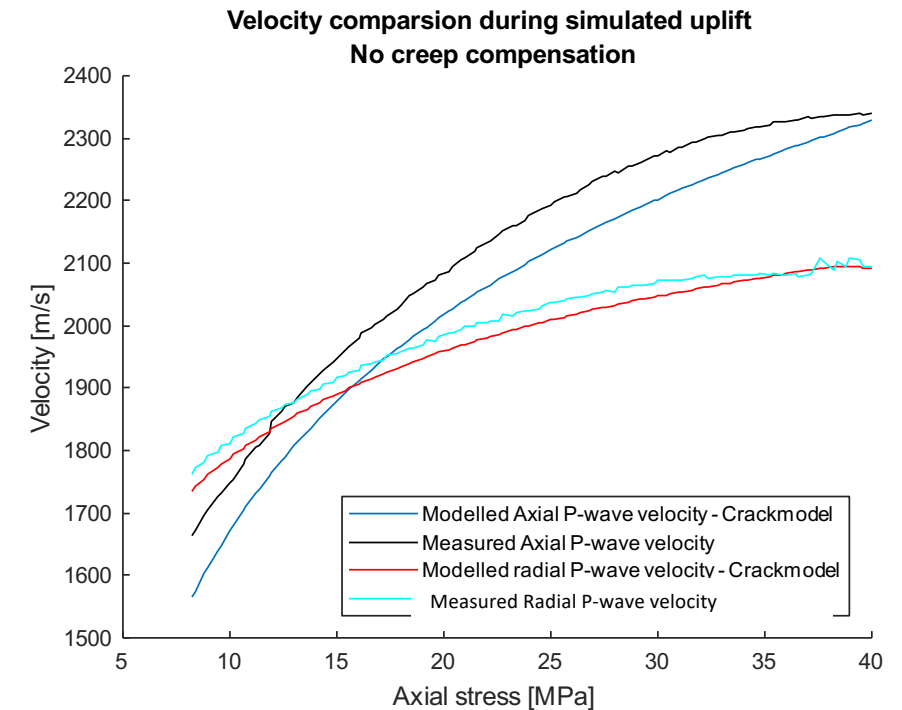
Modelling the uplift interval velocities

- The crack model presented in Fjær (2006) was tested (among others) to attempt to model the observed velocity changes

- This model has three parameters (n, β, η) describing stress sensitivity due to normal stress and shear deformation

- The green curves are made by fitting n, β and η using a Levenberg-Marquardt fit of the measured velocities with the measured stress and strains.

- It was concluded that the crack model could describe the uplift interval in the experiment.

Modelled Axial P-wave velocity

Measured axial P-wave velocity: Unloading ("Uplift")
Modelled axial P-wave velocity: Unloading ("Uplift")

Modelled Radial P-wave velocity

Measured radial P-wave velocity ("Uplift")
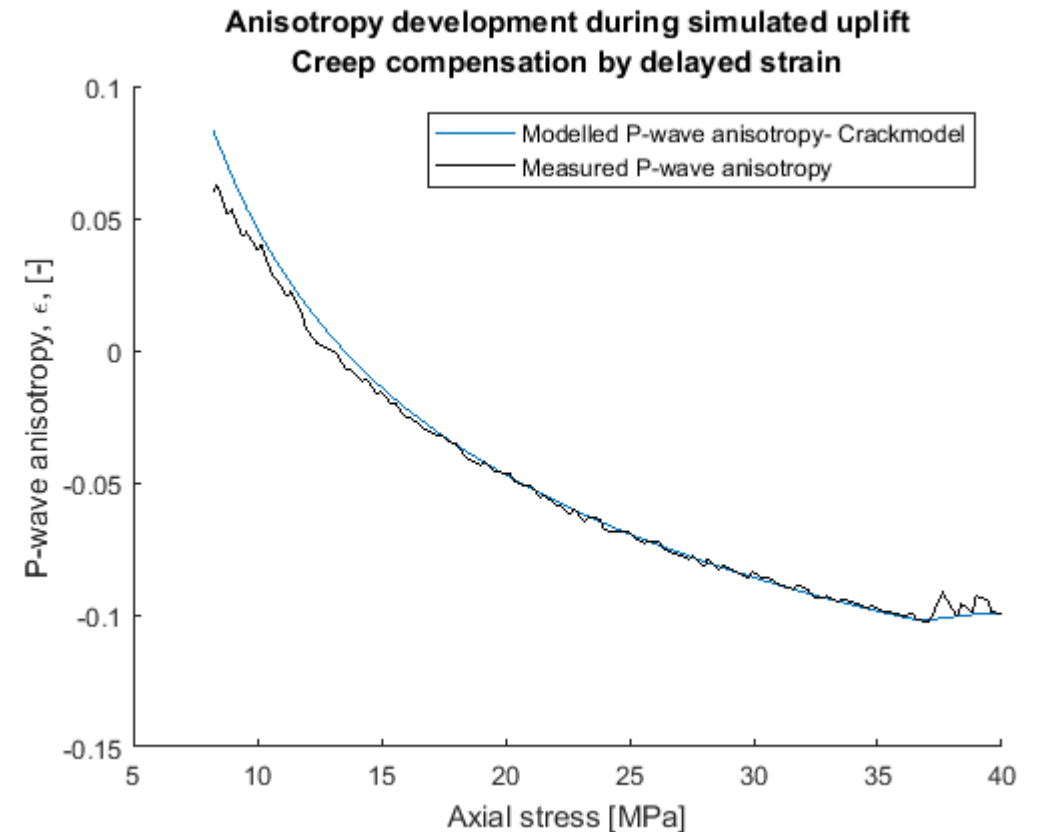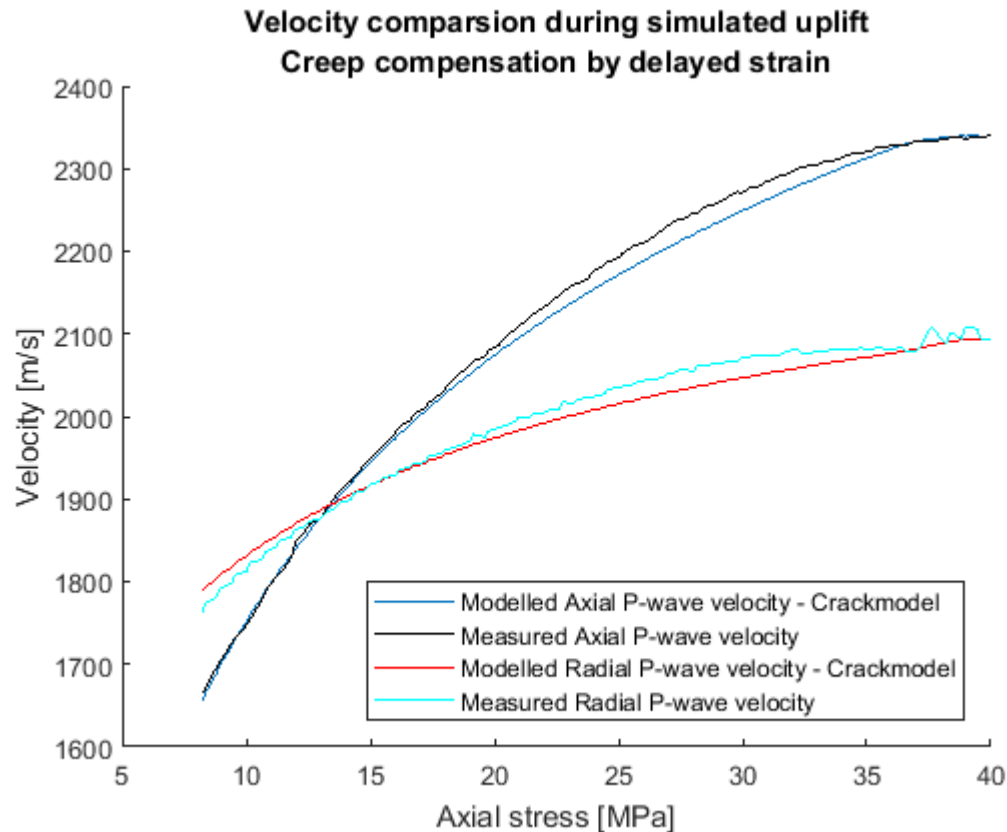Modelled radial P-wave velocity ("Uplift")

Modelling Uplift

- Strain is generally not available in the field
- Instead of using the experimental strain, an iteration loop for small changes in stress using the generalised Hooke's law is utilized to estimate input strain in the model
- Inputs needed are thus:
  - Stress
  - Velocity at the start of uplift
  - Porosity and Density
- Captures the trend at late stages of uplift, but over predicts stress sensitivity at the start of uplift

- Since experimental strain is not used, the effect of creep is ignored by the model – continued compactional strain would delay velocity decrease in the crack model.

Velocity comparsion during simulated uplift
No creep compensation

Axial stress vs Axial strain

Pragmatic compensation for delayed strain

Velocity comparsion during simulated uplift
Creep compensation by delayed strain

Velocity [m/s] vs Axial stress [MPa]

- Modelled Axial P-wave velocity - Crackmodel
- Measured Axial P-wave velocity
- Modelled Radial P-wave velocity - Crackmodel
- Measured Radial P-wave velocity

Anisotropy development during simulated uplift
Creep compensation by delayed strain

P-wave anisotropy, ϵ, [-] vs Axial stress [MPa]

- Modelled P-wave anisotropy- Crackmodel
- Measured P-wave anisotropy

For these curves the measured velocity is used, but to model the entire burial history requires modelling of the phases prior to uplift

Pre-cementation loading (Granular media)

- Walton (1987) developed relations between stiffness, strain and stress for granular media consisting of infinitely rough or smooth contacts
  - Explicit expressions for two strain states states: Uniaxial and Hydrostatic strain
- In the experiment, during this phase the loading is conducted with $\sigma_z = 2\sigma_r$ - Neither uniaxial nor hydrostatic strain.
- Bandyopadhyay (2009) developed expressions for a biaxial strain scenario, with a basis in Walton (1987) but with some (suspected) errors and a limit on the strain anisotropy
- A new model with ideas from Bandyopadhyay (2009) has been made, but correcting the (suspected) mistakes and with no limitation on strain anisotropy

Post-cementation loading

- A model capable of describing both anisotropy and stress dependence in cemented rocks is required.

- The patchy cement model described in Avseth et al. (2016) can describe stress sensitivity but not anisotropy.

- The model in Avseth et al. (2016) uses an isotropic granular media as the lower bound, but by using an anisotropic granular media instead, the anisotropy can be preserved

- The cemented rock stiffness is obtained using the model in Dvorkin and Nur (1996)

- The mixing is done using an anisotropic Hashin-Shtrikman formulation found in Parnell and Calvo-Jurado (2015)
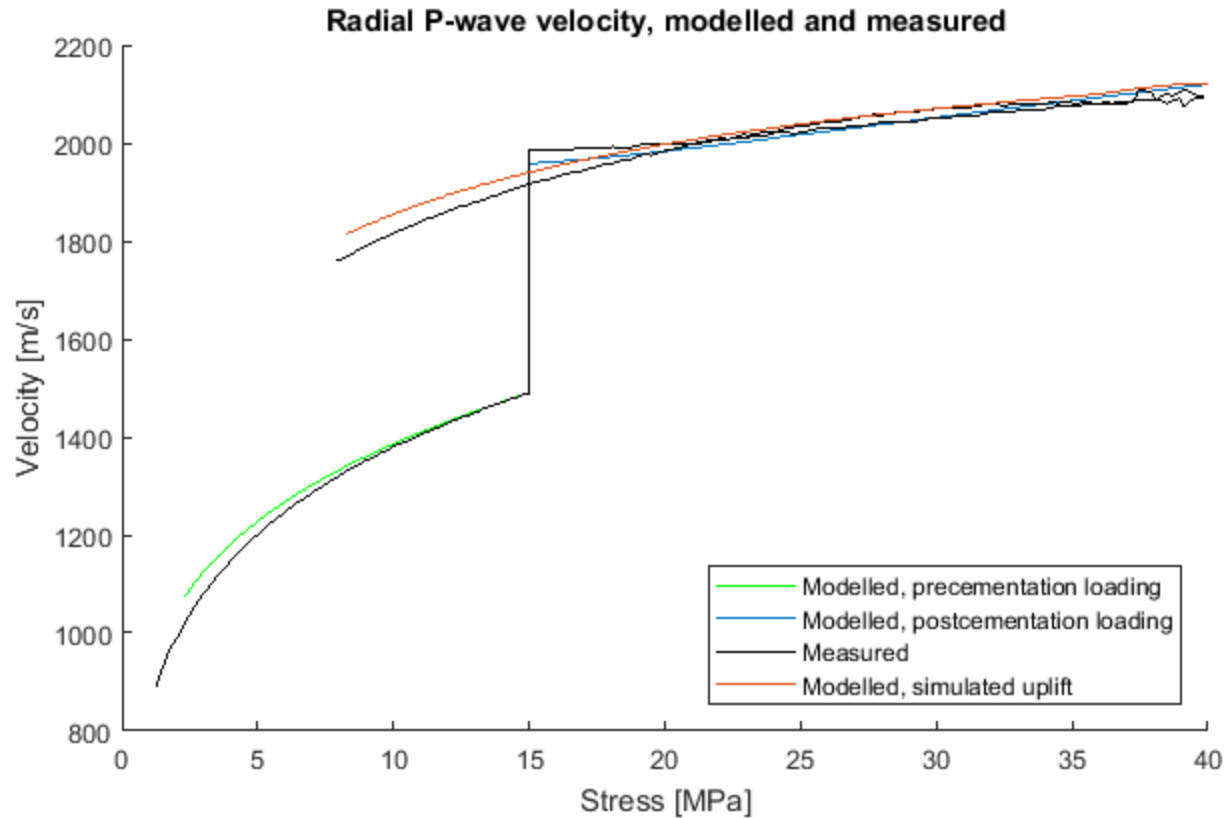
Final result

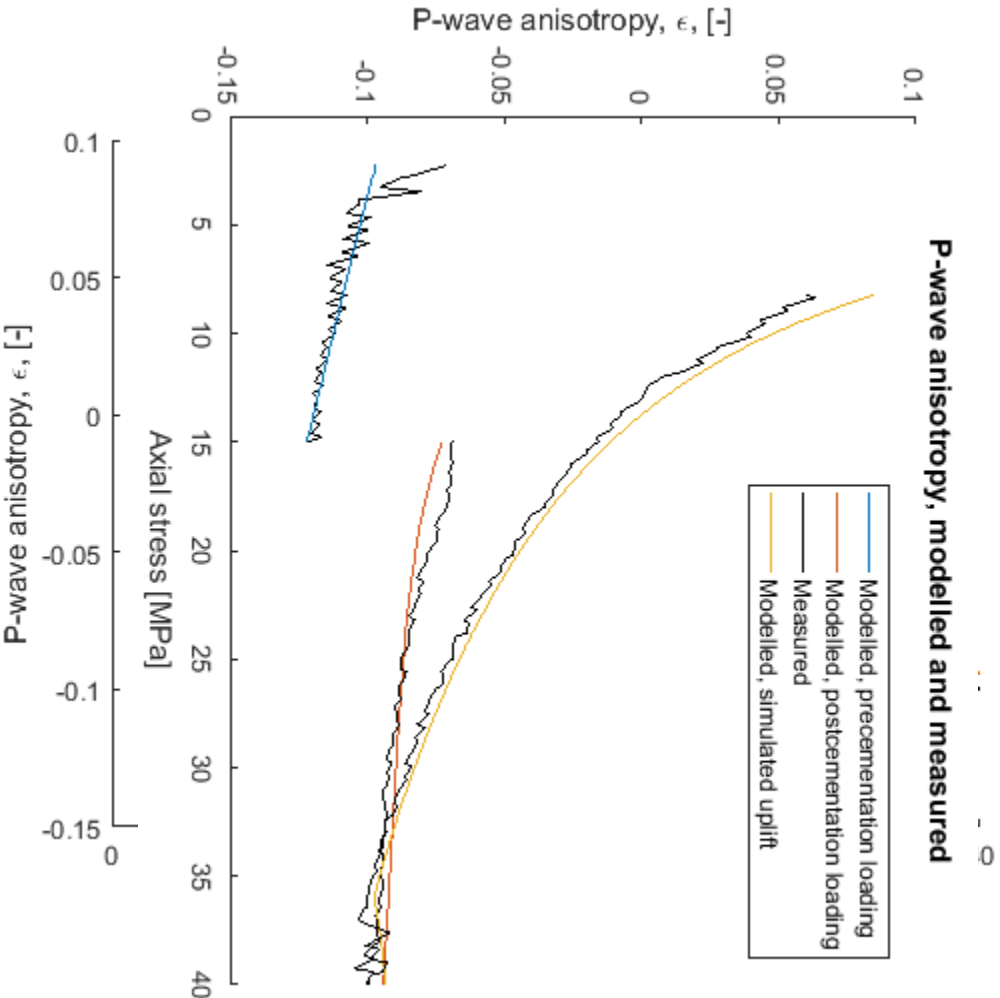- The three models can then be combined to one continous burial history

Final overview Axial P-wave velocity

Axial P-wave velocity, modelled and measured
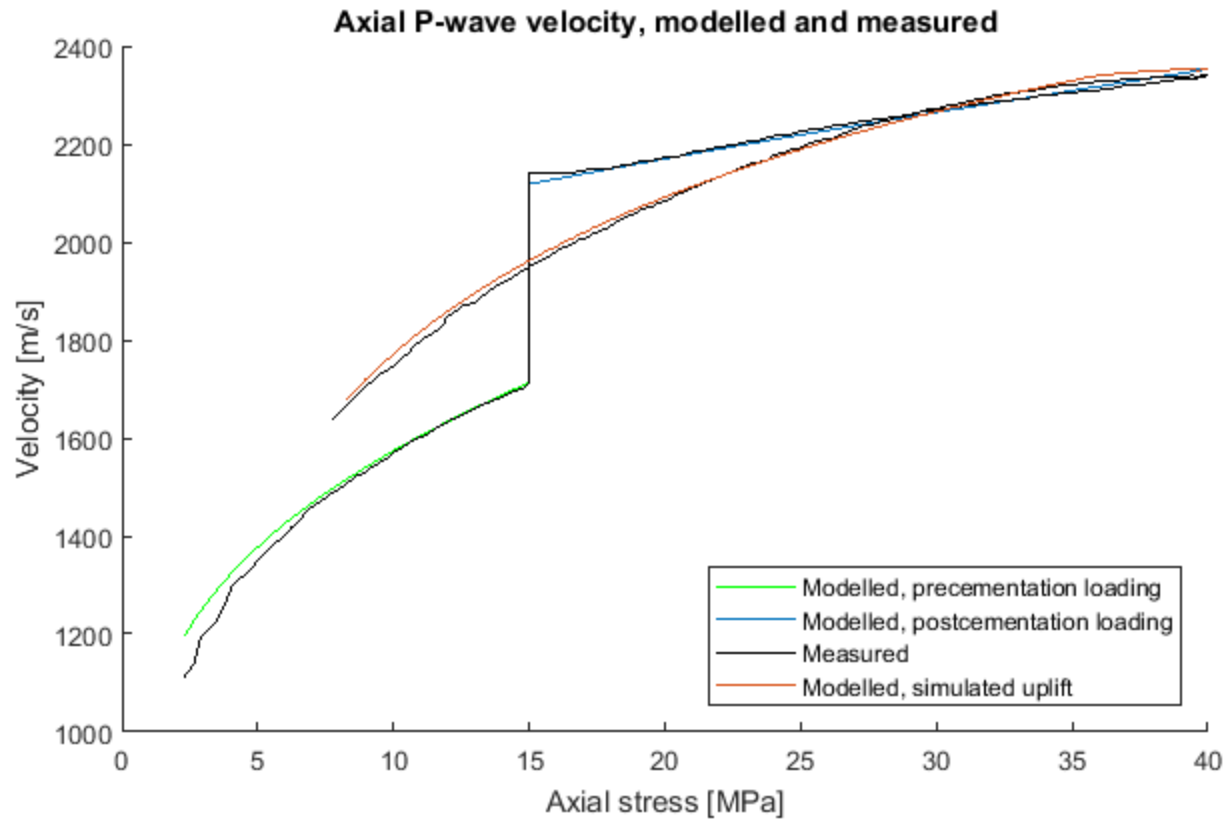
Final overview: Radial P-wave velocity

Radial P-wave velocity, modelled and measured

Final Overview - Anisotropy

Limitations and assumptions – could be a pressentation of its own – Quick overview

- Lab setup – How translatable are these results to the field case:
  - Temperature – higher temperature in the field -> More ductile
  - Strain rate – Higher in the lab
  - Uniaxial strain during uplift?
- Granular media models
  - All the assumptions in Walton (1987)
  - Mixing of rough and smooth contacts
- Cementation models (Anisotropic Patchy Cement)
  - The assumption that the rock can be seen as a mixture of cemented (whose stiffness is determined based on Dvorkin and Nur (1996)) and uncemented grain contacts (whose stiffness is determined by the methodology developed in this work, based on Avseth et al. (2016)).
- Crack model
  - In the model presented here limited to uniaxial strain.
  - Small enough stress and strain $\rightarrow$ Generalised Hooke's law in iteration loop with the crack model
  - Creep in the experimental data can be compensated.

Summary

- The experiments suggest an increased stress dependence during uplift.

- Under uniaxial strain conditions there is also a change in the P-wave anisotropy during simulated uplift compared to burial

- These laboratory tests have been used to test a rock physics model that for a set of input parameters models the Axial and Radial P-wave velocities (and thus the P-wave anisotropy) during burial and uplift.

- Plethora of limitations and assumptions

References

Avseth, P., Skjei, N., Mavko, G., 2016. Rock-physics modeling of stress sensitivity and 4d time shifts in patchy cemented sandstones—application to the visund field, north sea. The Leading Edge 35 (10), 868–878.

Bandyopadhyay, K., 2009. Seismic anisotropy: Geological causes and its implications to reservoir geophysics. Stanford University.

Dvorkin, J., Nur, A., 1996. Elasticity of high-porosity sandstones: Theory for two north sea data sets. Geophysics 61 (5), 1363–1370.

Dvorkin, J., Nur, A., Yin, H., 1994. Effective properties of cemented granular materials. Mechanics of materials 18 (4), 351–366.

Fjær, E., 2006. Modeling the stress dependence of elastic wave velocities in soft rocks. In: Golden Rocks 2006, The 41st US Symposium on Rock Mechanics (USRMS). American Rock Mechanics Association.

Holt, R., Brignoli, M., Kenter, C., 2000. Core quality: quantification of coring-induced rock alteration. International Journal of Rock Mechanics and Mining Sciences 37 (6), 889–907.

Holt, R., Stenebråten, J., Brignoli, M., et al., 2014. Effects of cementation on in situ and core compaction of soft sandstone. In: 48th US Rock Mechanics/Geomechanics Symposium. American Rock Mechanics Association.

Parnell, W. J., Calvo-Jurado, C., 2015. On the computation of the hashin–shtrikman bounds for transversely isotropic two-phase linear elastic fibre-reinforced composites. Journal of Engineering Mathematics 95 (1), 295–323.

Walderhaug, O., 1996. Kinetic modeling of quartz cementation and porosity loss in deeply buried sandstone reservoirs. AAPG bulletin 80 (5), 731–745.

Walton, K., 1987. The effective elastic moduli of a random packing of spheres. Journal of the Mechanics and Physics of Solids 35 (2), 213–226.

Extra

Biaxial Walton (rough)

$$\epsilon_{ij} = \epsilon_{11}\delta_{1i}\delta_{1j} + \epsilon_{11}\delta_{2i}\delta_{2j} + \epsilon_{33}\delta_{3i}\delta_{3j}$$

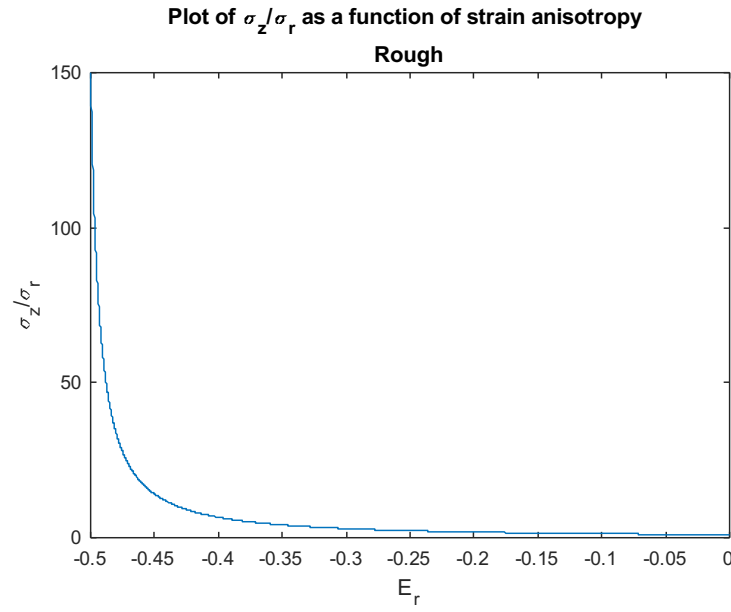$$\sigma^r_{11} = Z \cdot (-2BE_{11}I_3 - C \cdot I_9) =$$
$$Z \cdot (-4BE_{33}(E_r + 0.5)I_3 - C \cdot I_9)$$

Create expressions for stress and stiffness in terms of 10 integral equations (same procedure as Bandyopadhyay, except the integrals are solved without assumptions)

$$E_r = \frac{E_{11}}{2E_{33}} - 0.5$$

$$\sigma^r_{33} = Z \cdot (-2BE_{33}I_4 - C \cdot I_{10}) =$$

$$C^r_{11} = X \cdot (4BI_3 + 2CI_1)$$

From Walton:

$$C_{ijkl} = \frac{3(1-\phi)N}{4\pi^2 B(2B+C)} \left\{ B\left[\langle (-E_{pq}n_p n_q)^{1/2} n_j n_k \rangle \delta_{ij} + \right. \right.$$
$$\langle (-E_{pq}n_p n_q)^{1/2} n_i n_k \rangle \delta_{jl} + \langle (-E_{pq}n_j n_l)^{1/2} \rangle \delta_{ik} +$$
$$\left. \langle (-E_{pq}n_i n_l)^{1/2} \rangle \delta_{jk} \right] + 2C \langle (-E_{pq}n_p n_q)^{1/2} n_i n_j n_k n_l \rangle \left. \right\}$$
$$(4)$$

$$C^r_{33} = X \cdot (4BI_5 + 2CI_2)$$

$$I_1 = \langle (E_{pq}n_p n_q)^{0.5} n_1^4 \rangle =$$
$$\frac{1}{4096} \frac{\sqrt{E_{33}}}{(-E_r)^{5/2}} [480(-E_r)^{5/2} - 64(-E_r)^{5/2} - 24\sqrt{-E_r} +$$
$$V \cdot (240\sqrt{2}E_r^3 + 72\sqrt{2}E_r^2 - 12\sqrt{2}E_r + 6\sqrt{2})]$$

$$C^r_{13} = X \cdot (2CI_6)$$

$$C^r_{44} = X \cdot (BI_4 + BI_5 + 2CI_7)$$

$$\sigma^r_{ij} = \frac{(1-\phi)N}{\pi^2 B(2B+C)} \left[B\langle (-E_{pq}n_p n_q)^{0.5}[E_{ik}n_k n_j + E_{jk}n_k n_i] \rangle \right.$$
$$\left. -C\langle (-E_{pq}n_p n_q)^{3/2} n_i n_j \rangle \right]$$

$$C^r_{66} = X \cdot (BI_3 + BI_4 + 2CI_8)$$

$$X = \frac{3(1-\phi N)}{4\pi^2 B(2B+C)}$$

Biaxial Walton (rough)

- Expressions for stress and strain can't (at least by me) be solved analytically..

- But.. Can Newton's method to solve an equation equal to zero

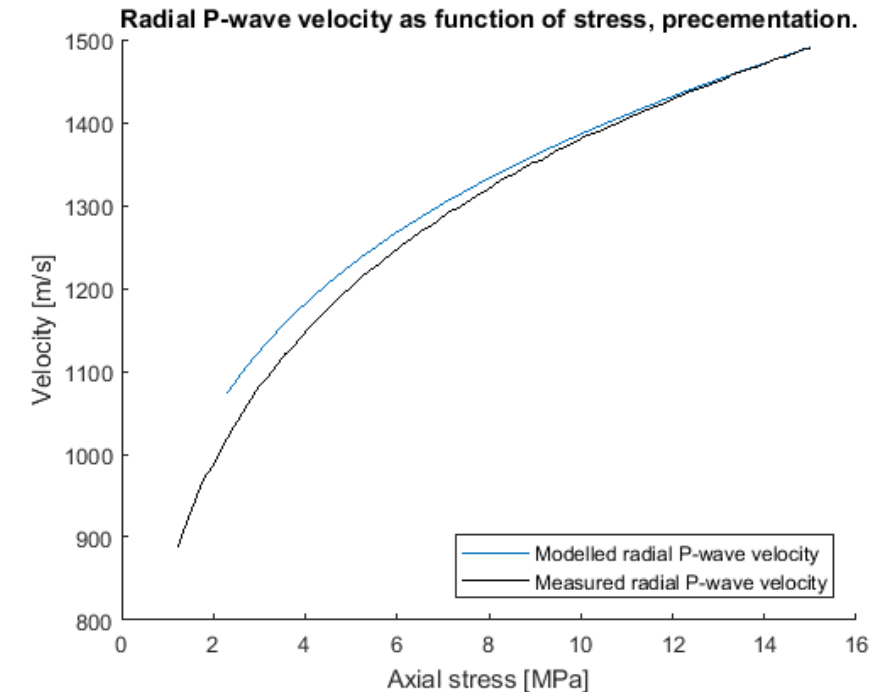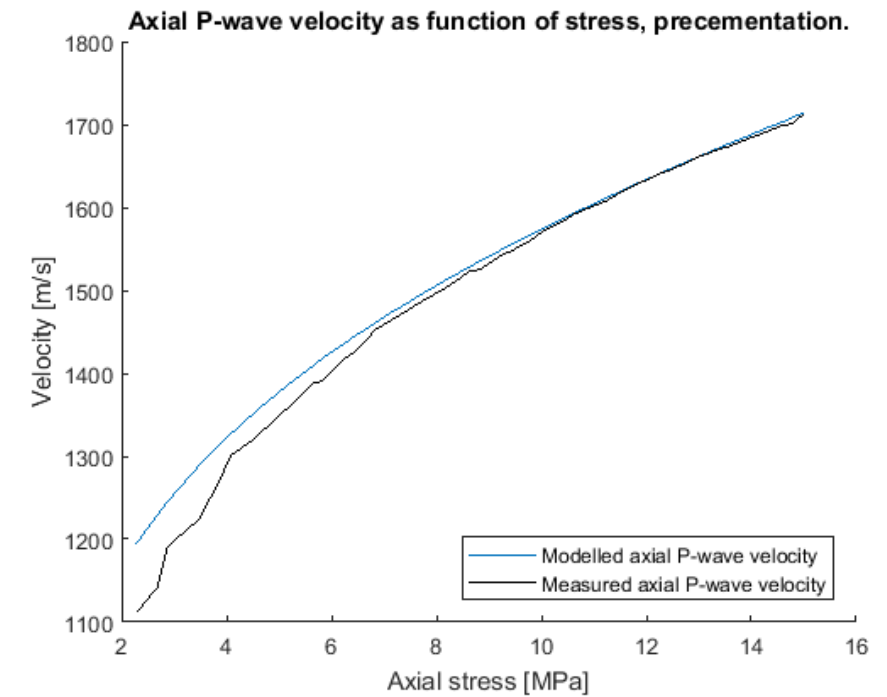- Very small σ_r in the limit of uniaxial compaction is a "limit" effect

The Newton method is ALWAYS linearly stable (but it may diverge if x_0 is sufficiently far from x_*) – not the case, know E_r between -0.5 and 0

$$f(E_r) = 2\left[24\,CE_r{}^3\sqrt{2}V + 48\,C(-E_r)^{5/2} + 48\,BE_r{}^2\sqrt{2}V + \right.$$
$$36\,CE_r{}^2\sqrt{2}V + 48\,BE_r\,\sqrt{2}V - 96\,B(-E_r)^{3/2} +$$
$$18\,CE_r\,\sqrt{2}V - 64\,C(-E_r)^{3/2} + 12\,B\sqrt{2}V + 3\,C\sqrt{2}V -$$
$$48\,B\sqrt{-E_r} - 12\,C\sqrt{-E_r}\right]/$$
$$\left[288\,BE_r{}^3\sqrt{2}V + 120\,CE_r{}^3\sqrt{2}V + 240\,C(-E_r)^{5/2} + \right.$$
$$240\,BE_r{}^2\sqrt{2}V + 576\,B(-E_r)^{5/2} + 108\,CE_r{}^2\sqrt{2}V +$$
$$24\,BE_r\,\sqrt{2}V - 384\,B(-E_r)^{3/2} + 18\,CE_r\,\sqrt{2}V$$
$$-\,176\,C(-E_r)^{3/2} - 12\,B\sqrt{2}V - 3\,C\sqrt{2}V + 48\,B\sqrt{-E_r} +$$
$$12\,C\sqrt{-E_r} - \frac{\sigma_{33}}{\sigma_{11}} = 0 \tag{56}$$

$$\frac{df(E_r)}{dE_r} = 144\left[96\,B^2\sqrt{2}E_r\,V + 12\,C^2\sqrt{2}E_r\,V + 8\,C^2\sqrt{2}E_r{}^2V - \right.$$
$$18\,BC\sqrt{-E_r}V^2 + 16\,C^2\sqrt{2}E_r{}^3V + 144\,BC(-E_r)^{3/2}V^2 +$$
$$64\,B^2\sqrt{2}E_r{}^2V + 768\,B^2\sqrt{2}E_r{}^4V + 96\,C^2\sqrt{2}E_r{}^4V +$$
$$128\,B^2\sqrt{2}E_r{}^3V + 576\,BC(-E_r)^{7/2}V^2 - 432\,BC(-E_r)^{5/2}V^2 -$$
$$288\,BC(-E_r)^{9/2}V^2 + 72\,C^2(-E_r)^{3/2} + 576\,B^2(-E_r)^{3/2} +$$
$$192\,B^2(-E_r)^{3/2}V^2 + 24\,C^2(-E_r)^{3/2}V^2 - 3\,C^2\sqrt{-E_r}V^2 +$$
$$432\,BC(-E_r)^{3/2} - 24\,B^2\sqrt{-E_r}V^2 + 72\,BC\sqrt{2}E_r\,V +$$
$$96\,BC\sqrt{2}E_r{}^3V + 48\,BC\sqrt{2}E_r{}^2V +$$
$$576\,BC\sqrt{2}E_r{}^4V - 768\,B^2(-E_r)^{7/2} -$$
$$160\,C^2(-E_r)^{5/2} - 1280\,B^2(-E_r)^{5/2} - 96\,C^2(-E_r)^{7/2} +$$
$$768\,B^2(-E_r)^{7/2}V^2 - 48\,C^2(-E_r)^{9/2}V^2 - 384\,B^2(-E_r)^{9/2}V^2 -$$
$$576\,BC(-E_r)^{7/2} - 960\,BC(-E_r)^{5/2} - 72\,C^2(-E_r)^{5/2}V^2 -$$
$$576\,B^2(-E_r)^{5/2}V^2 + 96\,C^2(-E_r)^{7/2}V^2\right]/$$
$$\left[(288\,BE_r{}^3V\sqrt{2} + 120\,CE_r{}^3V\sqrt{2} + 240\,BE_r{}^2V\sqrt{2} + \right.$$
$$108\,CE_r{}^2V\sqrt{2} + 576\,B(-E_r)^{5/2} + 24\,BE_r\,V\sqrt{2} +$$
$$240\,C(-E_r)^{5/2} + 18\,CE_r\,V\sqrt{2} - 384\,B(-E_r)^{3/2} -$$
$$12\,BV\sqrt{2} - 176\,C(-E_r)^{3/2} - 3\,CV\sqrt{2} +$$
$$48\,B\sqrt{-E_r} + 12\,C\sqrt{-E_r})^2\sqrt{-E_r}\right]$$

Plot of σ_z/σ_r as a function of strain anisotropy
Rough

Results

- The model uses a combination of rough and smooth contacts, as suggested in Bandyopadyhay (2009) ++
- In addition, information regarding the grains (coordination number, shear modulus and Poission's number) is needed
- There also exists a parameter that in essence has a similar effect as to make the rough/smooth relationship anisotropic and stress dependent
  - Based on the argument that as stress increases the number of rough contacts will increase, and as the loading is not isotropic, this effect will be anisotropic → In essence a fitting parameter for anisotropy
- Shear wave velocity for this set of parameters is overpredicted

Axial P-wave velocity as function of stress, precementation.

Radial P-wave velocity as function of stress, precementation.

Results

- Radial P-wave velocity stress-sensitivity somewhat overpredicted.
- Cement volume in the sample is not actually known exactly (this was not an important parameter for SINTEF), but the amounts are small, and the figures are modelled with a cement volume close to 2%

APC: Anisotropic Patchy Cement

Axial P-wave velocity - APC

Radial P-wave velocity - APC